Interocular suppressive interactions in amblyopia depend on spatial frequency.

Marie Beleyrian, Robert F. Hess, Frederic Matonti, Danièle Denis, Frédéric Chavane, Alexandre Reynaud

Vision Research 168 (2020) 18–28

Contents lists available at ScienceDirect

Vision Research

journal homepage: www.elsevier.com/locate/visres

Interocular suppressive interactions in amblyopia depend on spatial frequency

Marie Beylerian[a,b], Robert F. Hess[c], Frédéric Matonti[b,d], Danièle Denis[a,b], Frédéric Chavane[b], Alexandre Reynaud[c,*]

[a] Department of Ophthalmology, CHU NORD, Marseille, France
[b] Institut de Neurosciences de la Timone (INT), Centre National de la Recherche Scientifique (CNRS) and Aix-Marseille Université (AMU), Marseille, France
[c] McGill Vision Research, Department of Ophthalmology and Visual Sciences, McGill University, Montreal, Quebec, Canada
[d] Centre Paradis Monticelli, Marseille, France

ARTICLE INFO

Keywords:
Contrast sensitivity
qCSF
Spatial frequency
Amblyopia
Dichoptic masking

ABSTRACT

In amblyopia, there is an interocular suppressive imbalance that results in the fixing eye dominating perception. In this study, we aimed to determine whether these suppressive interactions were narrowband and tuned for spatial frequency or broadband and independent of spatial frequency.

We measured the contrast sensitivity and masking functions of fifteen amblyopic subjects and seventeen control subjects using the *quick Contrast Sensitivity Function (qCSF)* approach (Lesmes, Lu, Baek, & Albright, 2010). We first measured the monocular sensitivity functions of each participant and thereafter corrected for it. We then measured masking sensitivity functions for low, mid and high spatial frequency masks, normalized to their visibility.

In the control group, we observed that the strength of dichoptic masking is equivalent between the two eyes. It is also tuned such that masking by low spatial frequencies in one eye mainly affects low spatial frequencies in the other eye and masking by high spatial frequencies mainly affects high spatial frequencies. In amblyopes, although the interocular masking is also tuned for spatial frequency, it is not equivalent between the two eyes: the masking effect from the amblyopic to fixing eye is weaker than the other way around.

The asymmetry observed in the strength of masking between the two eyes in amblyopia is tuned for spatial frequency. It is not the consequence of the contrast sensitivity deficit of the amblyopic eye nor is it the consequence of abnormally strong masking from the fixing eye. Rather it is due to an abnormally weak masking strength by the amblyopic eye *per se*.

1. Introduction

Amblyopia represents a neurodevelopmental disorder of the visual cortex that is initiated by an early disruption of visual information processing during the critical period of maturation. The anatomical and functional developments of visual pathways and brain areas involved in visual perception are not complete at birth. As a consequence, during this critical period, visual perception is vulnerable to any early disruption of the visual experience. Amblyopes have reduced vision in one eye. Under binocular viewing, information from the two eyes does not both reach perception, there is a suppression of amblyopic eye information. Clinically, this is termed amblyopic suppression and it is an obstacle to reinstating binocular vision in these patients even when the acuity has been improved (Levi, Harwerth, & Smith, 1980; Zhou et al., 2018). The extent of this suppression, where it occurs in the cortex and the underlying mechanisms are not well understood (Barnes, Hess, Dumoulin, Achtman, & Pike, 2001; Kauffmann, Ramanoël, & Peyrin, 2014; Sengpiel, Jirmann, Vorobyov, & Eysel, 2006).

Binocular combination involves not only combination of the signals from the two eyes but also balanced inhibitory interactions (Ding & Sperling, 2006; Meese, Georgeson, & Baker, 2006). A starting point for understanding amblyopic suppression lies in these inhibitory binocular interactions which, in normals, are balanced to ensure optimal binocular combination (Ding & Sperling, 2006; Meese et al., 2006). Severely imbalanced binocular inhibition could form the basis of amblyopic suppression (Ding, Klein, & Levi, 2013; Zhou, Huang, & Hess, 2013). This simple explanation involving just the imbalance was originally suggested by Harrad and Hess (1992). They hypothesized that the

* Corresponding author.
E-mail address: alexandre.reynaud@mail.mcgill.ca (A. Reynaud).

https://doi.org/10.1016/j.visres.2019.11.008
Received 8 May 2019; Received in revised form 30 August 2019; Accepted 21 November 2019
Available online 08 February 2020

raised threshold in the amblyopic eye might be sufficient in itself to ensure suppression at all suprathreshold contrasts (that is contrasts that are multiples of the contrast threshold), based on the fact that the strength of masking depends on the *suprathreshold* contrast not the physical contrast (Legge, 1979). They went on to show that while this might explain the suppression in a subset of amblyopes, it did not provide a unique explanation for all amblyopes. Since then, there have been a number of studies (Huang, Baker, & Hess, 2012; Zhou et al., 2014; Levi, Waugh, & Beard, 1994), most notably that of Baker, Meese, and Hess (2008) that are consistent with what is now known as the attenuator explanation of suppression, namely weaker dichoptic masking of the fixing eye by the amblyopic eye due to an early signal attenuation (characterized by the reduced contrast sensitivity of the amblyopic eye).

A recent study (Zhou et al., 2018) provided a comprehensive test of this hypothesis by measuring dichoptic masking in normals and amblyopes using masks that were of equal suprathreshold contrast, designed to compensate for any early signal attenuation in the amblyopic eye. They argued that the signal attenuation explanation of suppression is only relevant at high spatial frequencies where the attenuation severely reduces the suprathreshold contrast range. At low-mid spatial frequencies, the signal attenuation in the amblyopic eye is either non-existent or minimal, yet suppression is still present even for masks that are designed to compensate for any monocular signal loss. Furthermore, suppression is of a greater magnitude at low-mid spatial frequencies. They showed that, in this spatial frequency range, suppression results from a net imbalance in the binocular inhibitory interactions underlying dichoptic masking; the inhibition from the fellow eye to the amblyopic eye, while being of normal magnitude, is larger than the abnormally reduced inhibition from the amblyopic to the fixing eye. They concluded that reduced contrast gain of the amblyopic eye rather than a simple signal attenuation (i.e. monocular contrast sensitivity deficit) underlies suppression. Recent studies of dichoptic masking at the cellular level (V1 and V2) in amblyopic monkey identified that the suppressive effects from the amblyopic eye were indeed reduced compared with that of the fellow fixing eye which were of a normal form (Hallum et al., 2017; Shooner et al., 2017). They also concluded that the visual pathway of the amblyopic eye exhibited a reduced contrast gain which would establish the mechanism underlying amblyopic suppression. Since all of their stimuli were of suprathreshold contrast, they were not able to rule out an explanation based solely on raised contrast thresholds.

So far, studies have focused on testing masking effects with masks at the same frequency as the target assuming that suppression is spatially tuned (Baker et al., 2008; Harrad & Hess, 1992; Kwon, Wiecek, Dakin, & Bex, 2015; Zhou et al., 2018). The alternative hypothesis is that suppression of the amblyopic eye does not follow the rules of normal dichoptic masking and results in a unitary displacement of sensitivity at all spatial frequencies. In this case, whether suppression occurs for a target of a particular spatial frequency viewed by the amblyopic eye will not depend on the spatial frequency of the target viewed by the fellow fixing eye. That amblyopic suppression is tuned for spatial frequency has been suggested by two earlier studies, one involving dichoptic masking (Levi, Harwerth, & Smith, 1979) and another concerning contrast adaptation (Hess, 1991). Levi et al. (1979) showed that like control subjects, amblyopes exhibit dichoptic interactions that are tuned for spatial frequency and orientation. Hess (Hess, 1991) showed that suppression prevented the amblyopic eye from adapting under binocular viewing unless each eye viewed a target of different spatial frequency or orientation. But it is hard to make general conclusions from these two studies as the number of subjects tested was small and the stimulus parameters were limited. There is a need to re-examine this issue on a larger number of amblyopes for equi-detectable stimuli spanning the whole spatial frequency range.

In the present study, we continue the practice of using masks (equi-detectable) that are designed to compensate for any early signal attenuation (masks of equal suprathreshold contrast for all conditions and all subjects) to answer the question as to whether these interocular suppressive interactions in amblyopia occur between cells tuned for similar spatial frequency or whether they are more global in nature and untuned for spatial frequency. We assess for the first time whether suppression is spatially tuned or not in the high, medium and low spatial frequency ranges for equi-detectable masks. We first measure the masking functions for three masks set at low, mid and high spatial frequencies and assess the spatial tuning of these masking effects in normals and amblyopes. Our test stimuli were Gabor patches whose detectability was measured using a qCSF approach (Lesmes, Lu, Baek, & Albright, 2010) which we have already adapted to dichoptic masking paradigms (Zhou et al., 2018). We used masks comprising 2-D bandpass (sum of 2 patterns filtered at orthogonal orientations, 1.8 octaves) filtered isotropic noise at one of three different peak spatial frequencies (0.25c/d, 1.31c/d, 4.93c/d). It is known in amblyopia that contrast well above threshold is perceived veridically by the amblyopic eye (Hess & Bradley, 1980; Loshin & Levi, 1983). In other words, above threshold, amblyopes can accurately match contrasts in their both eyes. Therefore, the approach we have taken is a conservative one in which the contrast of mask stimuli is set to be the same factor above threshold in order to best account for the threshold loss in amblyopia and to equate masking stimuli. Hence, we first measured the detectability of a 1-D version of our noise patterns (noise pattern filtered at 1 given orientation) for each of the three peak spatial frequencies. All masks contrasts were then set to a constant factor above their detection threshold (5x threshold) for all conditions and for all subjects.

2. Methods

2.1. Subjects

Fifteen amblyopic subjects (9 females, mean age 35 ± 19) and seventeen control subjects (two authors, 10 females, mean age 32 ± 4) with normal or corrected-to-normal vision and normal stereo vision (TNO < 120″) participated in this study. The clinical details of the amblyopic subjects are reported in Table1. This research adhered to the tenets of the Declaration of Helsinki. Informed consent was obtained from the subjects after explanation of the nature and possible consequences of the study.

2.2. Apparatus

Stimuli and experimental procedures were programmed with Matlab R2015a (© the MathWorks) using the Psychophysics (Brainard, 1997; Kleiner et al., 2007; Pelli, 1997) and qCSF (Lesmes et al., 2010) toolboxes running on a Linux Ubuntu system. Stimuli were displayed on a wide passive 3D LG 32LB650V 32″ monitor, linearized, 1920x1080px, 60 Hz. The stereo image input was in top-down DVI format and was displayed in interleaved line stereo mode: the Left eye image was displayed in even scanlines and the right eye image was displayed in odd scanlines. The subjects viewed the stimuli at a viewing distance of 120 cm, in scotopic conditions, with passive polarized 3D glasses so that the left image was only seen by the left eye and the right image by the right eye.

2.3. Procedures

2.3.1. Alignment procedure

To avoid image misalignment, for strabismic subjects, a pre-test alignment procedure was performed. The subjects had to align two bars, seen by each eye respectively, in the center of the screen, by pressing the keyboard keys (up, down, right and left). The coordinates of the two bars were then used to display the stimuli in the two eyes in the following measures.

Table 1
Clinical details of amblyopic subjects. VA: visual acuity; Strab: strabismus; Aniso: anisometropia; NAE: nonamblyopic eye; AE: amblyopic eye; R: right; L: left; exo: exotropia; eso: esotropia; H: Hypertropia; TNO: Stereoscopic vision test in seconds of arc, NP: not perceived.

Subjects	Age	Gender	Type	Eye	Refraction	VA	Squint	History	TNO
S1	63	M	Strab	AE NAE	0.25–0.75 (−0.25 5°)	20/400 20/20	L : H 1°	Not patched	NP
S2	68	F	Strab	AE NAE	2.50 (−1.00 105°) 2.25 (−0.50 85°)	20/50 20/20	R : eso 3°	Not patched	NP
S3	25	F	Aniso	NAE AE	0.25–0.75 (−0.25 5°)	20/20 20/63		Patched during 1 year (unknown duration)	480
S4	35	F	Mixed	AE NAE	3.25 (1.75 65°) 2.50 (−1.50 115°)	20/32 20/20	R : eso 4°	Patched during 3 years (all day)	NP
S5	10	M	Aniso	AE NAE	−3.25(−5.50 5°) 0.25 (-3.00 170°)	20/40 20/20		Not patched	
S6	27	M	Strab	AE NAE	1.00 (−1.75 20°) 0.75 (−2.00 180°)	20/32 20/20	R : eso 4°	Not patched	NP
S7	25	F	Strab	NAE AE	−2.50(−2.00 15°) −3.00(−3.25 170°)	20/20 20/50		Patched during 1 year (unknown duration); surgical treatment for strab	NP
S8	40	F	Mixed	AE NAE	3.50 (−0.50 115°) 0.25 (−0.25 180°)	20/32 20/20	R : eso 2°	Not patched	NP
S9	48	M	Aniso	AE NAE	0.50 (−2.25 15°) −0.25 (−0.50 155°)	20/25 20/20		Patched during 4 years (all day)	480
S10	64	M	Aniso	NAE AE	3.25 4.75 (−1.00 85°)	20/16 20/25		Not patched	NP
S11	11	F	Aniso	NAE AE	1.50 (−1.00 85°) 0.75 (−0.50 160°)	20/16 20/25		Patched during 1 year (unknown duration)	480
S12	43	F	Aniso	AE NAE	−9.25 (−1.00 65°) −1.00 (−0.25 110°)	1/100 20/20		Patched during 1 year (unknown duration)	480
S13	31	M	Mixed	NAE AE	0.00 (0.75 165°) 3.25 (−1.50 165°)	20/20 1/100		Surgical treatment for strab	NP
S14	12	F	Aniso	NAE AE	−1.50 (−0.50 140°) 2.25 (1.50 180°)	20/16 20/25		Not patched	120
S15	21	F	Aniso	NAE AE	−0.25(−2.00 20°) −6.75 (−2.50 55°)	20/20 20/50		Not patched	NP

2.3.2. The quick contrast sensitivity function (qCSF)

The monocular and masked contrast sensitivity functions were measured using the quick Contrast Sensitivity Function (*qCSF*) approach (Lesmes et al., 2010) in the spatial frequency range from 0.25c/d to 4.93c/d. This method is a Bayesian adaptive procedure that estimates the contrast sensitivity as a function of spatial frequency with a truncated log-parabola model (Watson & Ahumada, 2005). The *qCSF* approach has already been validated for its use on amblyopic populations (Gao et al., 2015; Hou et al., 2010).

A single interval identification task was used to estimate the detection sensitivity. For each trial, the stimulus frequency and contrast are set in order to maximize the expected information gain about the contrast sensitivity function (Lesmes et al., 2010). A trial time course was as follows: a red fixation dot was displayed on the screen, then the dot disappeared and the test stimulus was presented at a given orientation: horizontal or vertical for 500 ms with an auditory signal. After that, a green dot appeared to indicate to the subject that a response was expected. The subject had to press on key 4 of the keyboard if the orientation of the test stimulus appeared horizontal and on key 8 if the orientation of the stimulus appeared vertical. Each series consisted of 150 trials preceded by 5 training trials presented with high contrast.

2.3.3. Monocular sensitivity functions

First, two monocular sensitivity functions where measured for each eye using sinusoidal gratings and oriented filtered noise pattern stimuli while the other eye saw a mean gray background (Fig. 1a). Oriented noise patterns were created by filtering a white noise with horizontally- or vertically-oriented Gabor filters with a half-response spatial frequency bandwidth of 1.84 octaves. Targets were presented in a gaussian aperture of $\sigma = 3°$.

2.3.4. Masked sensitivity functions

Second, dichoptic masked contrast sensitivity functions were measured with the qCSF for each eye while a mask was presented dichoptically to the other eye. The target stimulus presented to the tested eye was a grating and the mask stimulus presented to the contralateral eye was a non-oriented random noise pattern created by summing two orthogonal patterns, as previously described (Fig. 1a). The *qCSF* was measured for 3 spatial frequencies of the mask: low-spatial frequency 0.25c/d (LSF), mid-spatial frequency 1.31c/d (MSF) and high-spatial frequency 4.93c/d (HSF). The contrast of the mask was set to five times

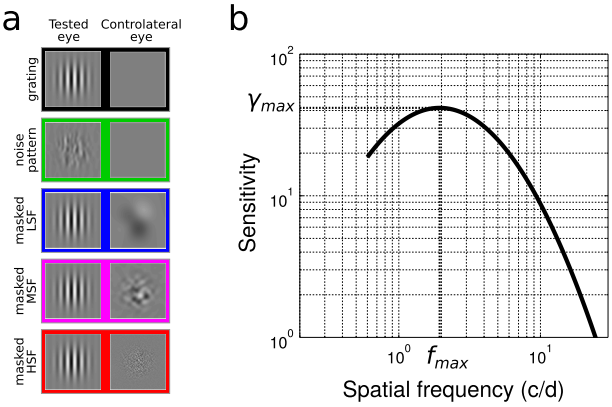

Fig. 1. Methods. a) Illustrations of stimuli configuration. From top to bottom: monocular grating detection (black), monocular oriented noise pattern detection (green), grating detection with a dichoptic low-spatial frequency mask presented in the controlateral eye (LSF, blue), grating detection with a dichoptic mid-spatial frequency mask (MSF, magenta) and grating detection with a dichoptic high-spatial frequency mask (HSF, red). b) Sensitivity function characterization. In the *qCSF* algorithm [1] the contrast sensitivity function is described by the truncated log-parabola model. Here we analyze only two of its parameters: the peak gain (γ_{max}) and the peak frequency. (For interpretation of the references to colour in this figure legend, the reader is referred to the web version of this article.)

its detection threshold (or 100% if ceiling was reached) as measured in the first step in order to factor out any signal attenuation. These thresholds are reported in Supplementary Tables 1 and 2 for control and amblyopic subjects respectively. Masks were presented in a gaussian aperture of $\sigma = 4.5^{\circ}$.

2.4. Data analysis

Data was analyzed off-line with Matlab R2017b (© the MathWorks) using the statistics and *qCSF* (Hess, 1991) toolboxes. The maximum gain γ_{max} and the peak frequencies f_{max} of the sensitivity functions were estimated by the *qCSF* procedure (Fig. 1b). To quantify the effect of the dichoptic masks on contrast sensitivity, we computed 4 masking indexes of the masking effect that a mask presented to one eye has on the sensitivity function of the contralateral eye for the 3 mask spatial frequencies. Thus, for instance the MI from the left eye corresponds to how much presenting a mask in the left eye influences the sensitivity of the right eye. They are calculated as the differences between the parameters of the monocular contrast sensitivity function and the 3 masked contrast sensitivity functions. The gain masking index (MI_{γ}) was defined as the logarithmic difference (in dB) between the maximum gain γ_{max} of the monocular and masked contrast sensitivity functions. The frequency-shift masking index (MI_f) was defined as the difference (in c/d) between the peak frequencies f_{max} of the functions. The low-frequency masking index (MI_l) and high-frequency masking index (MI_h) were defined as the logarithmic difference (in dB) between the monocular and dichoptic sensitivities at low (0.25c/d) and high (4.93c/d) spatial frequencies respectively.

For statistical analysis, we used a non-parametric Wilcoxon signed-rank test because the data could not be assumed to be normally distributed. In particular, to test the computed masking indexes were significantly different from 0, we used a two-sided Wilcoxon signed rank test ($\alpha = 0.001$). We tested if the masking indexes were significantly different between the two eyes with a paired two-sided Wilcoxon signed rank test ($\alpha = 0.05$).

3. Results

3.1. Control group

First, we measured monocular sensitivity function for each eye while the other eye viewed a mean gray background. For both eyes, the average contrast sensitivity to detect a grating peaks around 3.5c/d at an amplitude of approximately 150 (black curves in Fig. 2a and b). The sensitivity to the noise pattern (green curves) is lower and tuned to lower frequencies with a peak around 2.5c/d at an amplitude of approximately 40. Individual data is reported in Fig. A1.

Then we investigated dichoptic masking in the control group (Fig. 2a and b). Dichoptic masking contrast sensitivity function were measured for each eye while a mask was presented to the other eye. We can observe that the masking by low spatial frequencies (LSF) mainly affects low spatial frequencies and shifts the sensitivity function towards high spatial frequencies (blue curves). The dichoptic masking by high spatial frequencies (HSF) mainly affects high spatial frequencies and shifts the function towards low spatial frequencies (red curves). Masking by mid spatial frequencies (MSF) has the effect of reducing the overall magnitude of the function without changing its tuning much (magenta curves). In this respect, our use of the *qCSF* method (Lesmes et al., 2010) constrains the sensitivity function to follow a bell shape. Hence it is not clear if the masking by MSF would have created a notch in the sensitivity function that we might have not been able to resolve. However, as the function is not constrained at its inferior and superior edges, the specific amplitude reductions we report at low and high spatial frequencies are accurately accounted for.

We can appreciate the tuning of the masking sustained by each eye more specifically by plotting the difference between monocular grating sensitivity and the 3 masking conditions for the left and right eye (Fig. 2c and d). In order to better quantify these effects, we computed 4 masking indexes of each spatial frequency mask in one eye on the sensitivity function of the contralateral eye (Fig. 3 side panels, see Methods). Opposite to the masking sustained by each eye presented in Fig. 2c and d, they characterize the masking that one eye's stimulation induces on the other eye's sensitivity. These masking indexes (MI) and their significance (Wilcoxon signed rank test, $\alpha = 0.001$) are reported in Fig. 3 for the three masking conditions. We can observe that both the mid and high spatial frequency masks incur a significantly large gain masking index (MI_{γ} Wilcoxon signed rank test, $\alpha = 0.001$, Fig. 3a) which means that the overall gain of the sensitivity is reduced. The negative and positive values of the frequency-shift masking index (MI_f) for the LSF and HSF characterize the respective shift towards high and low spatial frequencies of the sensitivity function previously observed, although this index is only significant in one condition (Wilcoxon signed rank test, $\alpha = 0.001$, Fig. 3b).

The specificity of the masking effect is observed as well on the low- and high-frequency masking indexes (MI_l and MI_h respectively), which basically correspond to the values of the masking effect in the contralateral eye at spatial frequencies 0.25c/d and 4.93c/d in Fig. 2c and d. The MI_l is huge and significant for LSF and MSF masking conditions whereas it is not significant for the HSF masking (Wilcoxon signed rank test, $\alpha = 0.001$, Fig. 3c) which means low-spatial frequencies detection is not affected by high-spatial frequency masks. On the other hand, the MI_h is large and significant for MSF and HSF masking conditions whereas it is not significant for the LSF (Wilcoxon signed rank test, $\alpha = 0.001$, Fig. 3d). This means that high-spatial frequencies detection

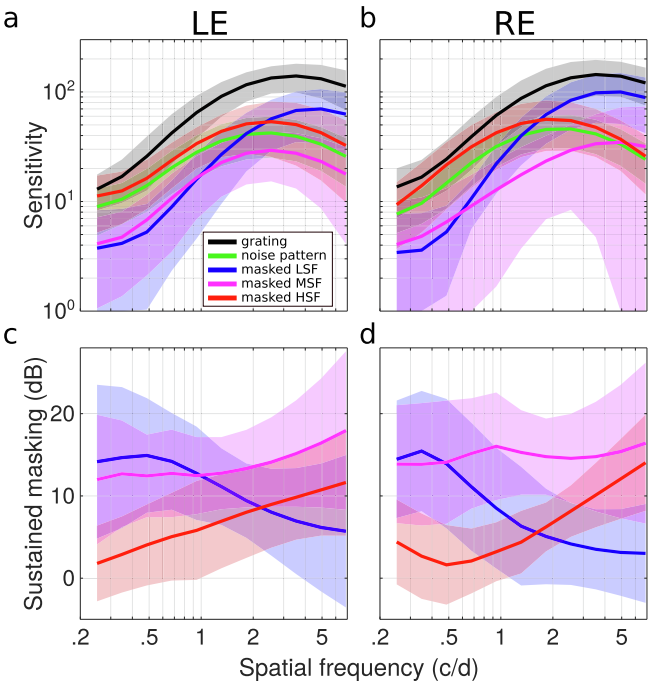

Fig. 2. Sensitivity functions and masking in the control group. a) Average sensitivity functions for each stimulus configuration for the left eye of the control group: monocular grating detection (black), monocular oriented noise pattern detection (green), grating detection with a dichoptic low spatial frequency mask presented in the contralateral eye (blue), grating detection with a dichoptic mid spatial frequency mask (magenta) and grating detection with a dichoptic high spatial frequency mask (red). b) same as a) for the right eye. c) Sustained masking induced on the left eye by the dichoptic low spatial frequency mask (blue), mid spatial frequency mask (magenta) and high spatial frequency mask (red). d) same as c) for the right eye. Shaded areas represent ± standard deviation. (For interpretation of the references to colour in this figure legend, the reader is referred to the web version of this article.)

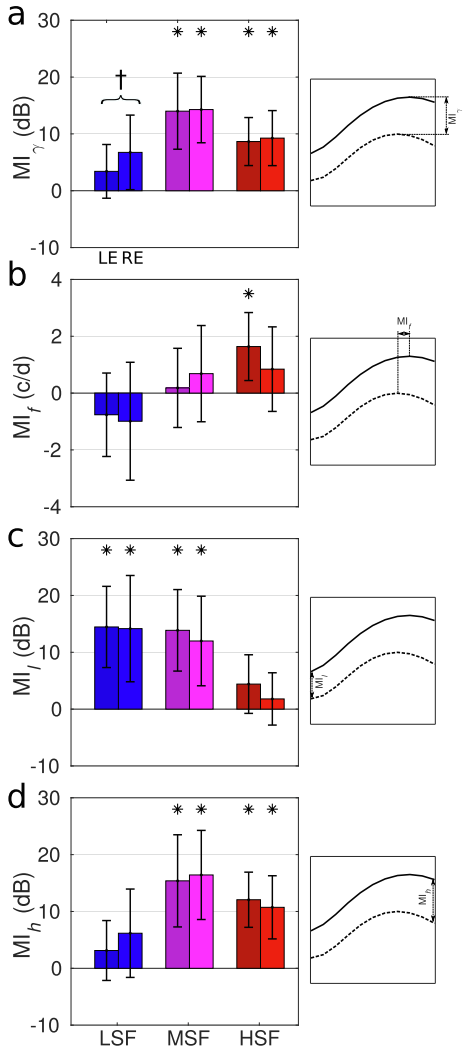

Fig. 3. Masking indexes in the control group. Each pair of bar represents the masking indexes from the left (LE, dark shades) and right (RE, normal shades) eye for the 3 dichoptic masks spatial frequencies: low (LSF, blue), mid (MSF, magenta) and high (HSF, red). Schematic representation of the masking indexes on the sensitivity curves are displayed in side panels. a) gain masking index (Mi_γ). b) frequency-shift masking index (MI_f), c) low-frequency masking index (MI_l). d) high-frequency masking index (MI_h). Error bars represent ± standard deviation. Asterisks indicate that masking indexes are significantly different from 0 (two-sided paired Wilcoxon signed rank test, $\alpha = 0.001$). Dagger indicates that masking indexes are significantly different between the two eyes (two-sided paired Wilcoxon signed rank test, $\alpha = 0.05$). (For interpretation of the references to colour in this figure legend, the reader is referred to the web version of this article.)

is not affected by low-spatial frequency masks. These observations confirm quantitatively and statistically that the dichoptic masking effect is coarsely tuned for spatial frequency.

Overall there is no laterality effect and there is no significant difference between the effect of the dichoptic mask on the 2 eyes (two-sided Wilcoxon signed rank test $\alpha = 0.05$, except on the MI_γ in the low-spatial frequency masking condition.

3.2. Amblyopic group

After assessing the tuning of dichoptic masking in the control group, we carried out a similar analysis in the amblyopic group. Individual data is reported in Fig. A2. Unlike in the control group, we can clearly see a big difference in the average contrast sensitivity between the

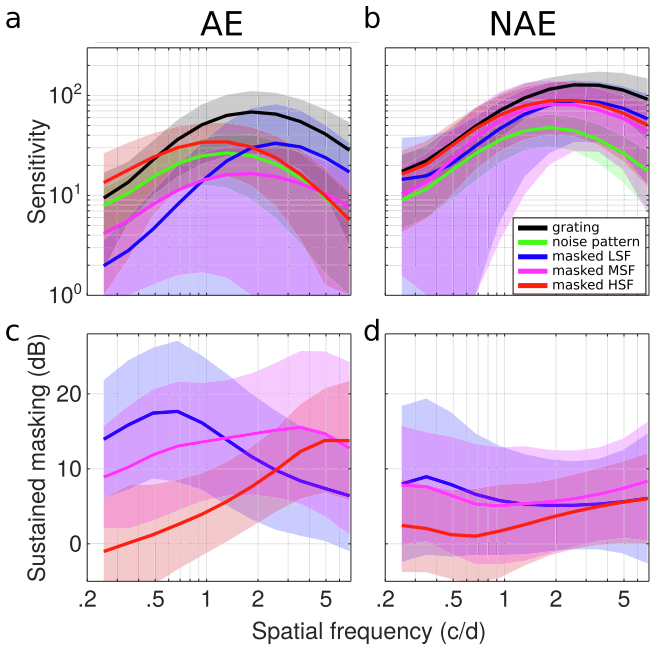

Fig. 4. Sensitivity functions and masking in the amblyopic group. a) Average sensitivity functions for each stimulus configuration for the amblyopic eye of the amblyopic group: monocular grating detection (black), monocular oriented noise pattern detection (green), grating detection with a dichoptic low spatial frequency mask presented in the controlateral eye (blue), grating detection with a dichoptic mid spatial frequency mask (magenta) and grating detection with a dichoptic high spatial frequency mask (red). b) same as a) for the non-amblyopic eye. c) Sustained masking induced on the amblyopic eye by the dichoptic low spatial frequency mask (blue), mid spatial frequency mask (magenta) and high spatial frequency mask (red). d) same as c) for the non-amblyopic eye. Shaded areas represent ± standard deviation. (For interpretation of the references to colour in this figure legend, the reader is referred to the web version of this article.)

amblyopic eye (AE) and the non-amblyopic eye (NAE, black curves in Fig. 4a and b). While the sensitivity to detect a grating or noise presented to the NAE is totally comparable to the sensitivity observed in the control group, the sensitivity of the AE is much lower and shifted towards lower spatial frequencies. The average grating contrast sensitivity peaks around 1.8c/d at an amplitude of approximately 70 for the amblyopic eye, whereas, for the non-amblyopic eye, it peaks around 3c/d at an amplitude of approximately 140.

Another difference comes from the fact that the sustained masking seems to be stronger in the AE than in the NAE. This can be appreciated by looking at the difference between monocular grating sensitivity and the 3 masking conditions for the amblyopic compared with that of the non-amblyopic eye in Fig. 4c and d. The sustained masking induced by the three spatial frequency masks on the AE is tuned and analogous to what is observed for controls (Fig. 2). However, the sustained masking on the NAE is weak and less tuned. This would mean that, contrary to what is observed in the control group, the suppressive effect between the NAE and AE is asymmetrical in the amblyopic group with the AE exerting an abnormally weak inhibitory influence on the NAE.

We quantified these effects by comparing the masking indexes from the AE and NAE and the masking indexes of the control group accumulated between the two eyes (CE), since there was not an eye difference (Fig. 5). However, we can note that some masking indexes which were not significant when the two eyes of the control group were analyzed separately became significant because of the double amount of data.

We can observe that the gain masking index MI_γ from the NAE is significant in the LSF and MSF conditions as in the control group, however it is not significant in any condition for the AE (Wilcoxon

signed rank test, α = 0.001, asterisks in Fig. 5a). And actually this effect is significantly different between the two eyes of the amblyopic group (two-sided paired Wilcoxon signed rank test, α = 0.05, daggers in Fig. 5a). The frequency-shift masking index MI_f from the NAE shows the same trend as in the control group, indicating that the dichoptic masking by the non-amblyopic eye generates a similar tuning shift on the amblyopic eye sensitivity function. However, it is not significant for the AE, which corroborates the lack of tuning of this weak masking (Wilcoxon signed rank test, α = 0.001, Fig. 5b). As in the control group, the low-frequency masking index MI_l from the NAE is huge and significant for LSF and MSF masking conditions. However, it is not significant for the HSF masking (Wilcoxon signed rank test, α = 0.001, asterisks in Fig. 5c) which again means low-spatial frequencies detection is not affected by high-spatial frequency masks. On the other hand, the high-frequency masking index MI_h from the NAE is high and significant for MSF and HSF masking conditions whereas it is not significant for the LSF (Wilcoxon signed rank test, α = 0.001, asterisks in Fig. 5d). This means that high-spatial frequencies detection is not affected by low-spatial frequency masks. This result confirms that the dichoptic masking by the non-amblyopic eye is tuned to similar frequencies as in the control group. For the amblyopic eye, none of the computed masking indexes were significant except the MI_h on mid-frequencies (Wilcoxon signed rank test, α = 0.001, asterisks in Fig. 5d) and this effect is significantly different compared to the non-amblyopic eye (two-sided paired Wilcoxon signed rank test, α = 0.05, daggers in Fig. 5d). This confirms that the amblyopic eye has a very weak and untuned masking influence on the non-amblyopic eye.

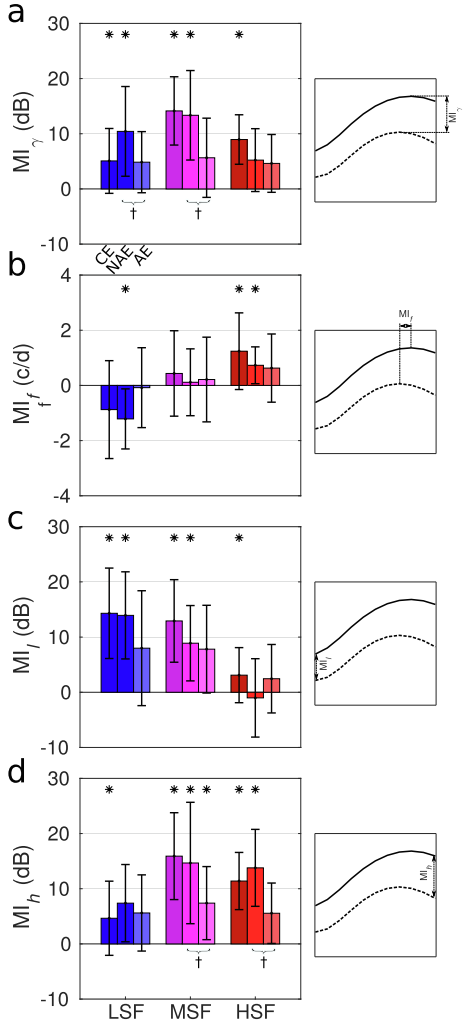

Fig. 5. Masking indexes in the amblyopic group. Each triplet of bar represents the masking indexes from the accumulated eyes of the control group (CE, dark shades) and the amblyopic (AE, standard shades) and non-amblyopic (NAE, light shades) eyes of the amblyopic group for the 3 dichoptic masks spatial frequencies: low (LSF, blue), mid (MSF, magenta) and high (HSF, red). Schematic representation of the masking indexes on the sensitivity curves are displayed in side panels. a) gain masking index (MI_γ). b) frequency-shift masking index (MI_f), c) low-frequency masking index (MI_l). d) high-frequency masking index (MI_h). Error bars represent ± standard deviation. Asterisks indicate that masking indexes are significantly different from 0 (two-sided paired Wilcoxon signed rank test, α = 0.001). Daggers indicate that masking indexes are significantly different between the AE and NAE of amblyopic subjects (two-sided paired Wilcoxon signed rank test, α = 0.05). (For interpretation of the references to colour in this figure legend, the reader is referred to the web version of this article.)

3.3. Correlation in the population

In order to test if this lack of influence is linked with the degree of amblyopia, we report in Fig. 6 the MI_γ as a function of the interocular visual acuity (VA) difference. In the LSF masking condition, the masking by the NAE (Fig. 6a) is stronger than by the AE (Fig. 6b) as previously observed and is not correlated with the VA difference. However, in the MSF and HSF masking conditions, these are negatively correlated (significant for the MSF in the AE and the HSF in both eyes:

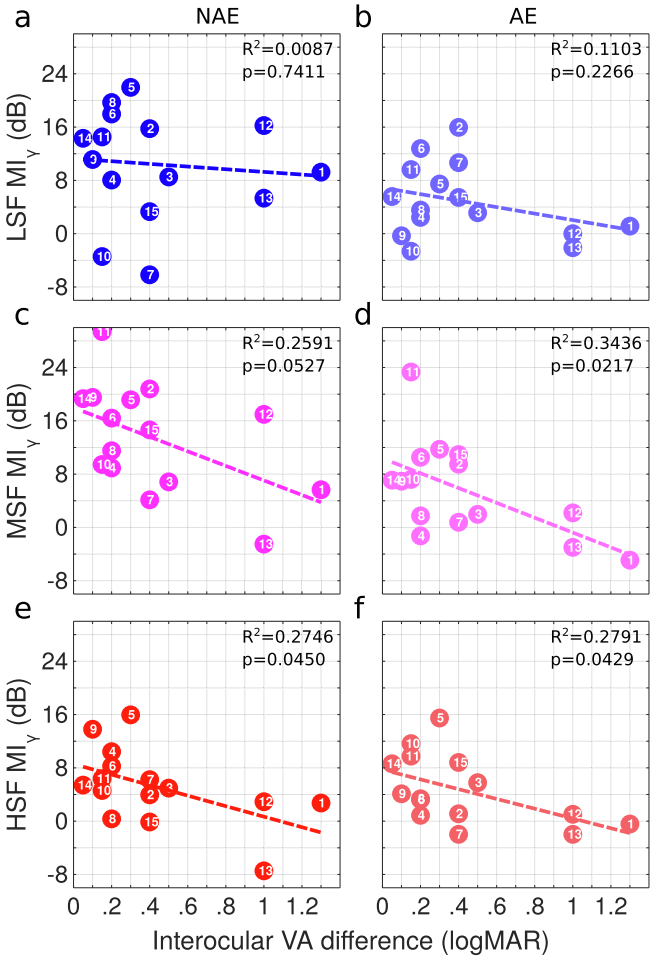

Fig. 6. Individual gain masking indexes MI_γ as a function of interocular visual acuity (VA) difference in the amblyopic group: with the low spatial frequency mask induced by the NAE (a) and the AE (b), for the mid spatial frequency mask induced by the NAE (c) and the AE (d) and for the high spatial frequency mask for the NAE (e) and the AE (f). Numbers report to individual amblyopic subjects in Table 1 and Appendix Fig. 2. Coefficients of determination r^2 and their respective p-values are reported in each panel.

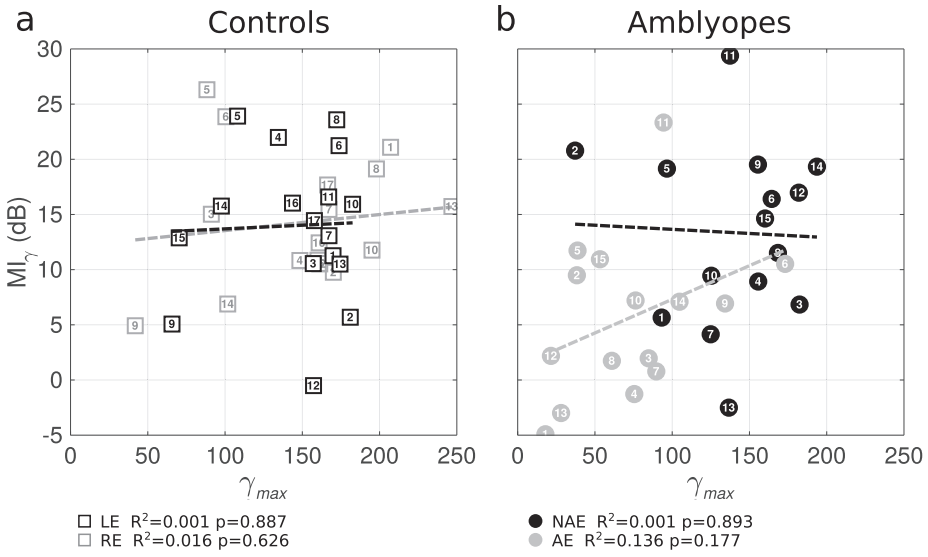

Fig. 7. Individual gain masking indexes MI_γ in the mid-spatial frequency masking condition as a function of the gain of the contrast sensitivity function γ_{max} in each eye. a) for the LE (black squares) and the RE (gray squares) of the control group. Numbers report to individual subjects as in Appendix Fig. 1. b) for the AE (gray circles) and the NAE (black circles) of the amblyopic group. Numbers report to individual amblyopic subjects in Table 1 and Appendix Fig. 2. Coefficients of determination r^2 and their respective p-values are reported for each eye, below panels.

Fig. 6d–f; almost significant for the NAE in the MSF condition: Fig. 6c; the coefficients of determination *r2* and their respective p-values are reported in each panel). Interestingly this is the case for both eyes. Thus, the presence of this correlation for the AE shows that the influence of the amblyopic eye on the non-amblyopic eye tends to decrease with the degree of amblyopia. More generally it indicates that a strong amblyopia, characterized by a large interocular VA difference, is associated with low masking indexes. Importantly, this weak interocular interaction occurs even though we have normalized all masks to be equi-detectable by both eyes regardless of the degree of amblyopia.

Another way to look at this interaction is to see how the masking generated by one eye depends on its threshold sensitivity. For this purpose, we plot the gain-masking index MI_γ for the mid-spatial frequency masking condition in each eye as a function of its sensitivity gain for both control and amblyopic subjects in Fig. 7. We only report this condition because it reflects how the peak sensitivity of the contrast sensitivity function changes without changing its tuning and as such is indicative of the global change of amplitude of the contrast sensitivity function. We can observe in the control group that for both eyes, the MI_γ of each eye is not correlated with its sensitivity gain (Fig. 7a). This could mean that, in normal conditions, the binocular interaction is a mechanism by itself, which works independently of each eye's threshold sensitivity. The same lack of correlation is observed for the non-amblyopic eye of the amblyopic group (Fig. 7b, black circles). However, there is a weak, though non-significant, correlation for the amblyopic eye which suggests that the amblyopic eye may exert a masking proportional to its threshold sensitivity, even though all stimuli were displayed at the same suprathreshold contrast (i.e. correcting for any difference in threshold sensitivity).

In order to investigate further the bilateral masking effects in the amblyopic population compared to the controls, we report for both of them the correlation between the gain-masking indexes of the two eyes for the mid-spatial frequency masking condition. That is, the MI_γ of the LE as a function of the MI_γ of the RE for controls and the MI_γ of the AE as a function of the MI_γ of the NAE for amblyopes (Fig. 8). So this plot is a direct comparison of the masking exerted by one eye compared to the other for each individual of each group. For both populations the correlation is strong and significant ($p < 0.05$). This suggests that the way the two eyes interact with each other depends on a common binocular mechanism. For the control population, this regression falls on the identity line which indicates that this mechanism is reciprocal in nature. However, for the amblyopic population the regression falls well below the identity line. This suggests that the interocular masking mechanism in the amblyopic system also represents a common interocular bidirectional mechanism but one that displays reduced masking strength by the amblyopic eye.

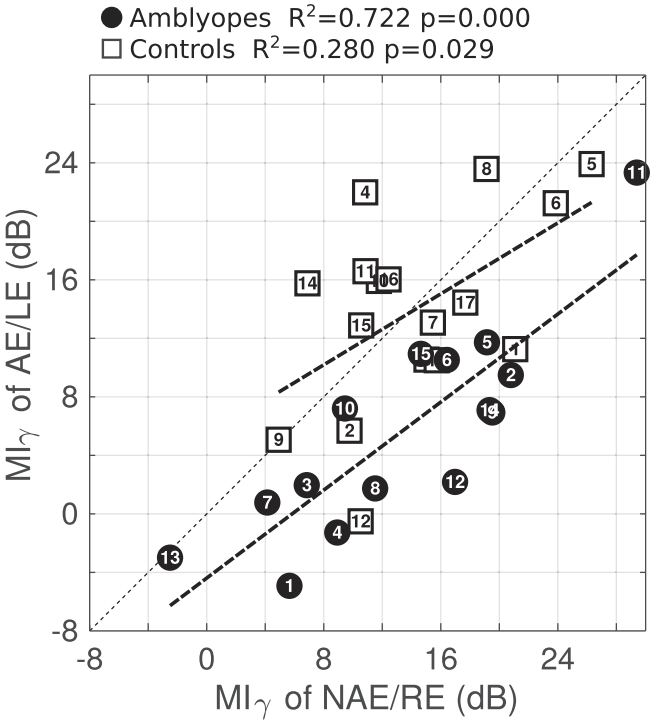

Fig. 8. Correlation between the gain masking indexes MI_γ in the MSF masking condition from the two eyes in the amblyopic and control groups. MI_γ induced by the LE as a function of the MI_γ of the RE in the control group (open squares, numbers report to individual control subjects in Fig. 6 and Appendix Fig. 1) an MI_γ from the AE as a function of the MI_γ from the NAE in the amblyopic group (full circles, numbers report to individual amblyopic subjects in Fig. 6, Table 1 and Appendix Fig. 2). Coefficients of determination r^2 and their respective p-values are reported for each group above the figure.

4. Discussion

A number of studies have shown that core amblyopic deficits such as contrast sensitivity loss are more marked at high spatial frequencies than at low spatial frequencies (Hess & Howell, 1977; Levi & Harwerth, 1977; Rentschler, Hilz, & Brettel, 1980; Sjöstrand, 1981) suggesting a

significant dependence on spatial frequencies in amblyopic vision. There is also evidence that threshold for binocular interactions (at detection threshold, when stimuli are barely detectable) show a dependence on spatial frequency (Ding et al., 2013; Kim, Reynaud, Hess, & Mullen, 2017), and that abnormal binocular interaction may be differentially affected by different spatial frequencies (Barrett, Pacey, Bradley, Thibos, & Morrill, 2003; Ding et al., 2013).

In this study, we assessed the tuning of dichoptic masking by assessing the effect one mask at a given spatial frequency, low, mid or high, has on the overall contrast sensitivity function in control and amblyopic subjects. In the control group, our results show that dichoptic masking by the LSF mask (0.25c/d) selectively reduces the sensitivity at low spatial frequencies and thus shifts the contrast sensitivity function tuning to higher spatial frequencies. On the other hand, dichoptic masking by the HSF mask (4.93c/d) selectively decreases the sensitivity at high spatial frequencies and shifts the contrast sensitivity function tuning to lower spatial frequencies (Fig. 2). Thus, dichoptic masking is spatial frequency tuned (Baker & Meese, 2007). In controls, these reciprocal interactions are balanced. For amblyopes, dichoptic masking by the non-amblyopic eye on the amblyopic eye (Fig. 4) is equivalent to dichoptic masking in the control group. It is tuned, normal in magnitude. A LSF mask will shift the contrast sensitivity function tuning to higher spatial frequencies and a HSF mask will shift the contrast sensitivity function tuning to lower spatial frequencies. On the other hand, the dichoptic masking by the amblyopic eye on the non-amblyopic eye is very weak and untuned. Although the reduced magnitude of masking for high spatial frequency in amblyopia has been previously reported (Zhou et al., 2018), the lack of spatial frequency tuning has not. This evidence for tuning of dichoptic masking from the non-amblyopic eye could have important implications for the development of binocular therapies. For example, removal of just high spatial frequency information from the non-amblyopic eye's image (e.g. Bossi et al., 2017) will not redress the dichoptic inhibitory balance that Zhou et al. (2018) revealed at low spatial frequencies since, as we show here, these inhibitory effects are spatially tuned. An overall reduction in the contrast of the non-amblyopic eye's image (Hess, Mansouri, & Thompson, 2010; To et al., 2011) that would affect all spatial frequencies would be, on the basis of the present results, a more effective strategy.

For amblyopes, dichoptic masking by the non-amblyopic eye on the amblyopic eye is tuned and normal in magnitude whereas dichoptic masking by the amblyopic eye on the non-amblyopic eye is very weak and untuned. We observe that the gain masking index MI_{γ} of the amblyopic eye is much smaller than the one of the NAE (Fig. 8). For the amblyopic eye this MI_{γ} is correlated with contrast sensitivity, whereas this is not the case for the non-amblyopic eye or for control eyes (Fig. 7). The two-stage model advanced by Meese et al. (2006) assumes a balance in the reciprocal interocular inhibition for binocular summation to operate optimally. However, as Harrad and Hess (1992) and later Baker et al. (2008) first pointed out, the strength of masking from the amblyopic eye will be impacted by its reduced contrast sensitivity and this factor will make a contribution to reducing the efficacy of binocular summation particularly at high spatial frequencies (Shooner et al., 2017). Although as we point out here, this is not the only factor (Baker et al., 2008; Chadnova, Reynaud, Clavagnier, & Hess, 2017; Reynaud & Hess, 2016).

Our conclusions for masks whose spatial frequency differs from that of the test stimuli are in agreement with those of the study of Zhou et al. (2018), who used masks and test stimuli that were matched in spatial frequency. In both studies the masks were all equi-detectable and both studies showed strong net masking disadvantaging the amblyopic eye, especially at low spatial frequencies where there are no or minimal threshold deficits (Harrad, 1996; Kim et al., 2017; Mower, Christen, Burchfiel, & Duffy, 1984). The present study's contribution is to show that this finding is also true for test and mask stimuli of different spatial frequency. Our results, for high spatial frequencies, are consistent with those of Baker et al. (2008) who demonstrated that the amblyopic eye signals only slightly influence the non-amblyopic eye in the spatial frequency range for which the detection threshold of the amblyopic eye is deficient. For these authors, the cause of the binocular deficit in amblyopia derives from the elevated monocular contrast detection threshold of the amblyopic eye (attenuation) and the amblyopic visual system can be represented approximately by normal dichoptic masking with unequal weights assigned to both eyes (Baker et al., 2008). They consider the nature of the suppression responsible for the deficits in amblyopia is passive, related to the degree of attenuation of the signal by the amblyopic eye (Baker et al., 2008; Zhou et al., 2014). Harrad and Hess (1992) have documented a number of possible forms that suppression might take in amblyopia, such as normal dichoptic masking (passive effects of amblyopic eye attenuation) or abnormal inhibitory interactions (active suppressive effects not accounted for by normal dichoptic interactions combined with amblyopic threshold attenuation). Moreover, they showed that these suppressive interactions depended on spatial frequency (being more marked at high spatial frequencies).

We observed that the strength of masking by MFS and HFS (Fig. 6) is correlated to the depth of amblyopia: the stronger the amblyopia, the smaller the masking initiated from the amblyopic eye. This is in agreement with the study by Li et al. (2011), who showed that the contrast needed in the non-amblyopic eye to achieve a binocular equilibrium point was lower in deep amblyopia, and therefore associated with a greater suppression. The significant correlation between the effect of masking on the amblyopic eye and the non-amblyopic eye demonstrates an asymmetry in dichoptic masking which is not directly the consequence of any threshold loss (Fig. 8). If we assume that the attenuation of the amblyopic eye is the only mechanism responsible for the lack of suppression and that the normalization to 5 times the detection thresholds we applied to the dichoptic masks should compensate for it, then the masking index in the NAE as a function of the AE in Fig. 8 should fall on the identity line for amblyopic subjects, as it does for controls. However, the masking index is higher for the NAE than the AE and these values lie below the identity line. Thus, this asymmetry rules out an explanation solely based on threshold attenuation in the interocular contrast gain control mechanism (Baker et al., 2008; Meese et al., 2006). Here, the notion of a reduced contrast gain associated with the inhibition of the fixing eye by the amblyopic eye is more attractive (Harrad & Hess, 1992; Harrad, 1996). Even though there is a correlation between the magnitude of this contrast gain deficit and the magnitude of the contrast loss at threshold, the latter is not directly responsible for the former. These suppressive effects could have a physiological basis in the inhibitory interactions between the two eyes inputs which take place in the primary visual cortex, as has been observed in cats and monkeys with surgically induced strabismus (Mower et al., 1984; Sengpiel et al., 2006; Shooner et al., 2017).

In conclusion, we observed that dichoptic masking is tuned for spatial frequency in normals and amblyopes. In amblyopia, the positive correlation between suppression and depth of amblyopia suggests that binocular dysfunction is the primary problem. The imbalance between the two eyes is not a consequence of the sensitivity loss but is correlated with a change in the contrast gain control that occurs a later stage in the amblyopic pathway.

Acknowledgments

The authors thank Dr Aurore Aziz, Dr Natacha Stolowy and Dr Lauren Sauvan for their help in recruiting the participants. This work was supported by a grant from the Agence Régionale de Santé Provence-Alpes-Côte d'Azur to MB, grants from the Canadian Institutes of Health Research (228103) and ERA-NET NEURON (JTC 2015) to RFH and by a FRQS Vision Health Research Network of Quebec networking grant to RFH, FC and AR.

Appendix

Appendix A. Individual subjects'data

Figs. A1 and A2

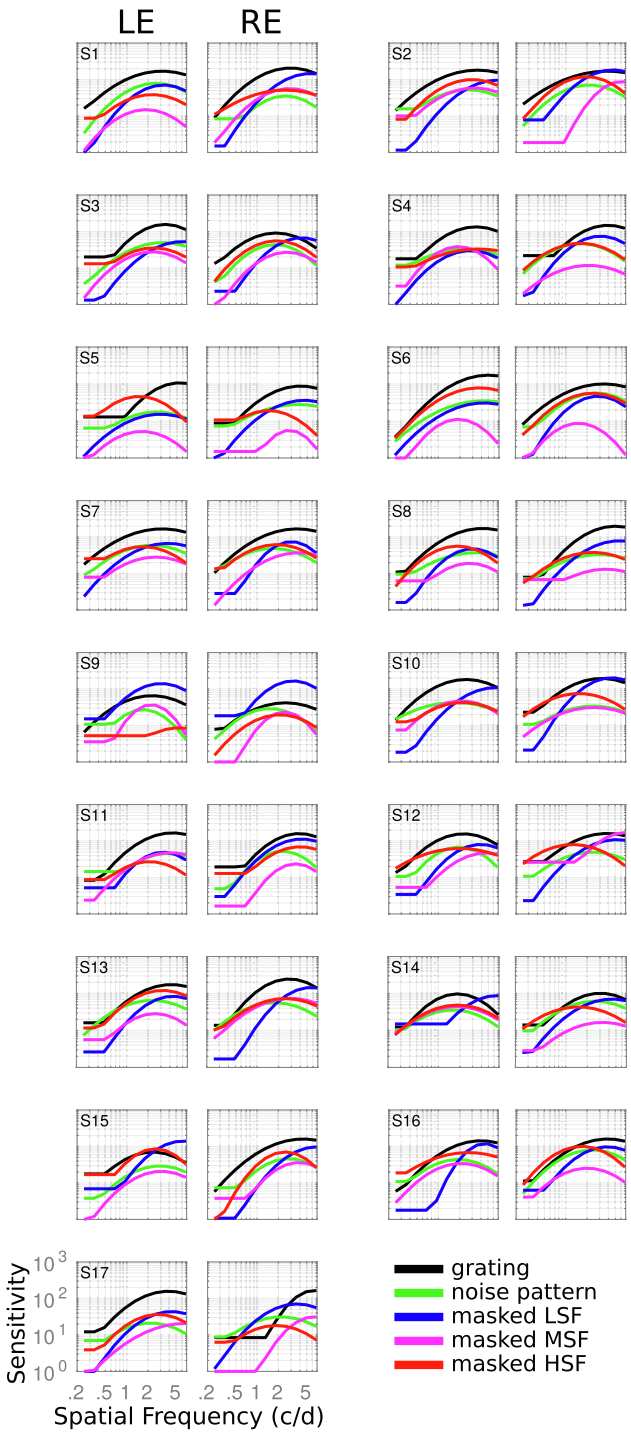

Fig. A1. Individual sensitivity functions of the control group. Each pair of panels represent the sensitivities of one subject, for the left eye (LE) in the left panel and the right eye (RE) in the right panel, for all stimulus configuration: monocular grating detection (black), monocular oriented noise pattern detection (green), grating detection with a dichoptic low spatial frequency mask presented in the controlateral eye (blue), grating detection with a dichoptic mid spatial frequency mask (magenta) and grating detection with a dichoptic high spatial frequency mask (red). (For interpretation of the references to colour in this figure legend, the reader is referred to the web version of this article.)

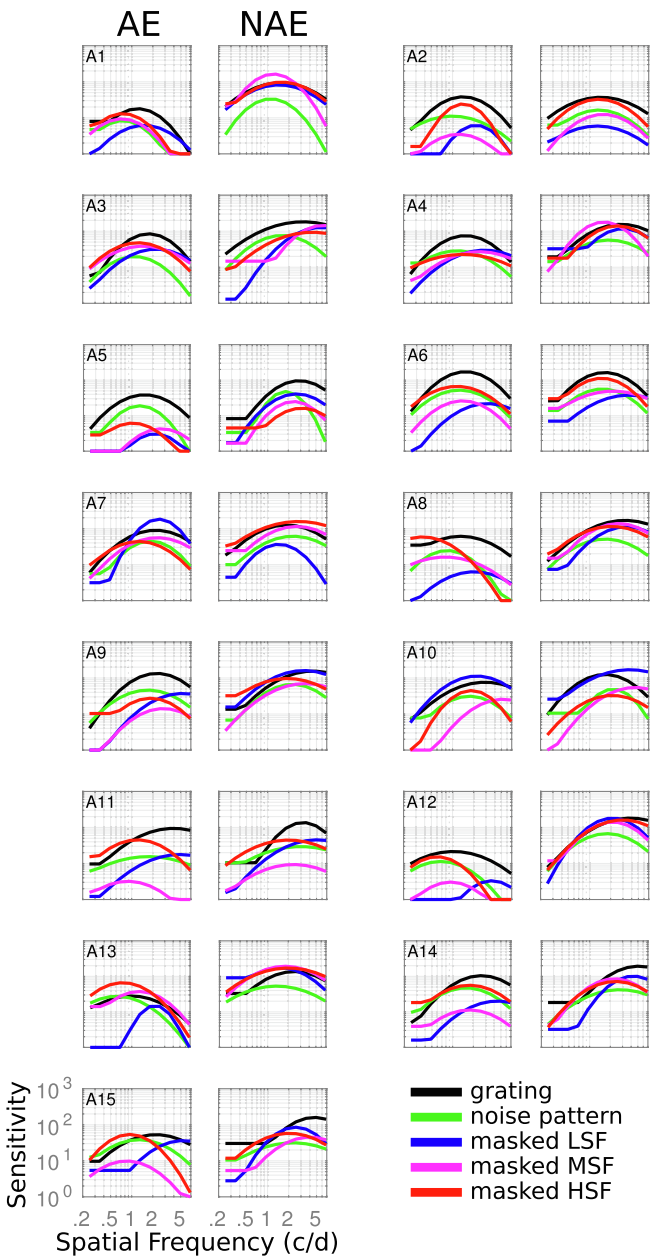

Fig. A2. Individual sensitivity functions of the amblyopic group. Each pair of panels represent the sensitivities of one subject, for the amblyopic eye (AE) in the left panel and the non-amblyopic eye (NAE) in the right panel, for all stimulus configuration: monocular grating detection (black), monocular oriented noise pattern detection (green), grating detection with a dichoptic low spatial frequency mask presented in the controlateral eye (blue), grating detection with a dichoptic mid spatial frequency mask (magenta) and grating detection with a dichoptic high spatial frequency mask (red). Numbers report to individual subjects as in Table 1. (For interpretation of the references to colour in this figure legend, the reader is referred to the web version of this article.)

Appendix B. Supplementary data

Supplementary data to this article can be found online at https://doi.org/10.1016/j.visres.2019.11.008.

References

Baker, D. H., & Meese, T. S. (2007). Binocular contrast interactions: Dichoptic masking is not a single process. *Vision Research, 47*, 3096–3107.

Baker, D. H., Meese, T. S., & Hess, R. F. (2008). Contrast masking in strabismic amblyopia: Attenuation, noise, interocular suppression and binocular summation. *Vision Research, 48*(15), 1625–1640.

Barnes, G. R., Hess, R. F., Dumoulin, S. O., Achtman, R. L., & Pike, G. B. (2001). The cortical deficit in humans with strabismic amblyopia. *Journal of Physiology, 533*(Pt 1), 281–297.

Barrett, B. T., Pacey, I. E., Bradley, A., Thibos, L. N., & Morrill, P. (2003). Nonveridical visual perception in human amblyopia. *Investigative Ophthalmology & Visual Science, 44*(4), 1555–1567.

Bossi, M., Tailor, V. K., Anderson, E. J., Bex, P. J., Greenwood, J. A., Dahlmann-Noor, A., et al. (2017). Binocular therapy for childhood amblyopia improves vision without breaking interocular suppression. *Investigative Ophthalmology & Visual Science, 58*, 3031–3043.

Brainard, D. H. (1997). The psychophysics toolbox. *Spatial Vision, 10*(4), 433–436.

Chadnova, E., Reynaud, A., Clavagnier, S., & Hess, R. F. (2017). Latent binocular function in amblyopia. *Vision Research, 140*, 73–80.

Ding, J., & Sperling, G. (2006). A gain-control theory of binocular combination. *Proceedings of the National Academy of Sciences of the United States of America, 103*(4), 1141–1146.

Ding, J., Klein, S. A., & Levi, D. M. (2013). Binocular combination in abnormal binocular vision. *Journal of Visualization, 13*(2), 14.
Gao, Y., Reynaud, A., Tang, Y., Feng, L., Zhou, Y., & Hess, R. F. (2015). The amblyopic deficit for 2nd order processing: Generality and laterality. *Vision Research, 114*, 111–121.
Hallum, L. E., Shooner, C., Kumbhani, R. D., Kelly, J. G., Garcia-Marin, V., Majaj, N. J., et al. (2017). Altered balance of receptive field excitation and suppression in visual cortex of amblyopic macaque monkeys. *Journal of Neuroscience, 37*(34), 8216–8226.
Harrad, R. (1996). Psychophysics of suppression. *Eye (London, England), 10*(Pt 2), 270–273.
Harrad, R. A., & Hess, R. F. (1992). Binocular integration of contrast information in amblyopia. *Vision Research, 32*(11), 2135–2150.
Hess, R. F. (1991). The site and nature of suppression in squint amblyopia. *Vision Research, 31*(1), 111–117.
Hess, R. F., & Bradley, A. (1980). Contrast perception above threshold is only minimally impaired in human amblyopia. *Nature, 287*(5781), 463–464.
Hess, R. F., & Howell, E. R. (1977). The threshold contrast sensitivity function in strabismic amblyopia: Evidence for a two type classification. *Vision Research, 17*(9), 1049–1055.
Hess, R. F., Mansouri, B., & Thompson, B. (2010). A new binocular approach to the treatment of amblyopia in adults well beyond the critical period of visual development. *Restorative Neurology and Neuroscience, 28*(6), 793–802.
Hou, F., Huang, C.-B., Lesmes, L., Feng, L.-X., Tao, L., Zhou, Y.-F., et al. (2010). qCSF in clinical application: Efficient characterization and classification of contrast sensitivity functions in amblyopia. *Investigative Ophthalmology & Visual Science, 51*(10), 5365–5377.
Huang, P.-C., Baker, D. H., & Hess, R. F. (2012). Interocular suppression in normal and amblyopic vision: Spatio-temporal properties. *Journal of Vision, 12*(11).
Kauffmann, L., Ramanoël, S., & Peyrin, C. (2014). The neural bases of spatial frequency processing during scene perception. *Frontiers in Integrative Neuroscience, 8*, 37.
Kim, Y. J., Reynaud, A., Hess, R. F., & Mullen, K. T. (2017). A normative data set for the clinical assessment of achromatic and chromatic contrast sensitivity using a qCSF approach. *Investigative Ophthalmology & Visual Science, 58*(9), 3628–3636.
Kleiner, M., Brainard, D., Pelli, D., Ingling, A., Murray, R., & Broussard, C. (2007). What's new in psychtoolbox-3. *Perception, 36*(14), 1–16.
Kwon, M., Wiecek, E., Dakin, S. C., & Bex, P. J. (2015). Spatial-frequency dependent binocular imbalance in amblyopia. *Scientific Reports, 5*, 17181.
Legge, G. E. (1979). Spatial frequency masking in human vision: Binocular interactions. *Journal of the Optical Society of America, 69*(6), 838–847.
Lesmes, L. A., Lu, Z.-L., Baek, J., & Albright, T. D. (2010). Bayesian adaptive estimation of the contrast sensitivity function: The quick CSF method. *Journal of Vision, 10*(3), 17.1-21.
Levi, D. M., Harwerth, R. S., & Smith, E. L. (1979). Humans deprived of normal binocular vision have binocular interactions tuned to size and orientation. *Science, 206*, 852–854.
Levi, D. M., Harwerth, R. S., & Smith, E. L. (1980). Binocular interactions in normal and anomalous binocular vision. *Documenta Ophthalmologica, 49*(2), 303–324.
Levi, D. M., Waugh, S. J., & Beard, B. L. (1994). Spatial scale shifts in amblyopia. *Vision Research, 34*(24), 3315–3333.
Levi, D. M., & Harwerth, R. S. (1977). Spatio-temporal interactions in anisometropic and strabismic amblyopia. *Investigative Ophthalmology & Visual Science, 16*(1), 90–95.
Li, J., Thompson, B., Lam, C. S., Deng, D., Chan, L. Y., Maehara, G., et al. (2011). The role of suppression in amblyopia. *Investigative Ophthalmology & Visual Science, 52*(7), 4169–4176.
Loshin, D. S., & Levi, D. M. (1983). Suprathreshold contrast perception in functional amblyopia. *Documenta Ophthalmologica, 55*(3), 213–236.
Meese, T. S., Georgeson, M. A., & Baker, D. H. (2006). Binocular contrast vision at and above threshold. *Journal of Vision, 6*(11), 1224–1243.
Mower, G. D., Christen, W. G., Burchfiel, J. L., & Duffy, F. H. (1984). Microiontophoretic bicuculline restores binocular responses to visual cortical neurons in strabismic cats. *Brain Research, 309*(1), 168–172.
Pelli, D. G. (1997). The VideoToolbox software for visual psychophysics: Transforming numbers into movies. *Spatial Vision, 10*(4), 437–442.
Rentschler, I., Hilz, R., & Brettel, H. (1980). Spatial tuning properties in human amblyopia cannot explain the loss of optotype acuity. *Behavioural Brain Research, 1*(5), 433–443.
Reynaud, A., & Hess, R. F. (2016). Is suppression just normal dichoptic masking? Suprathreshold considerations. *Investigative Ophthalmology & Visual Science, 57*(13), 5107–5115.
Sengpiel, F., Jirmann, K.-U., Vorobyov, V., & Eysel, U. T. (2006). Strabismic suppression is mediated by inhibitory interactions in the primary visual cortex. *Cerebral Cortex, 16*(12), 1750–1758.
Shooner, C., Hallum, L. E., Kumbhani, R. D., García-Marín, V., Kelly, J. G., Majaj, N. J., et al. (2017). Asymmetric dichoptic masking in visual cortex of amblyopic macaque monkeys. *Journal of Neuroscience, 37*(36), 8734–8741.
Sjöstrand, J. (1981). Contrast sensitivity in children with strabismic and anisometropic amblyopia. A study of the effect of treatment. *Acta Ophthalmologica, 59*(1), 25–34.
To, L., Thompson, B., Blum, J. R., Maehara, G., Hess, R. F., & Cooperstock, J. R. (2011). A game platform for treatment of amblyopia. *IEEE Transactions on Neural Systems and Rehabilitation Engineering, 19*, 280–289.
Watson, A. B., & Ahumada, A. J. (2005). A standard model for foveal detection of spatial contrast. *Journal of Vision, 5*(9), 717–740.
Zhou, J., Huang, P.-C., & Hess, R. F. (2013). Interocular suppression in amblyopia for global orientation processing. *Journal of Vision, 13*(5), 19.
Zhou, J., McNeal, S., Babu, R. J., Baker, D. H., Bobier, W. R., & Hess, R. F. (2014). Time course of dichoptic masking in normals and suppression in amblyopes. *Investigative Ophthalmology & Visual Science, 55*(7), 4098–4104.
Zhou, J., Reynaud, A., Yao, Z., Liu, R., Feng, L., & Zhou, Y. (2018). Amblyopic suppression: Passive attenuation, enhanced dichoptic masking by the fellow eye or reduced dichoptic masking by the amblyopic eye? *Investigative Ophthalmology & Visual Science, 59*(10), 4190–4197.